Preprints.org

Article

Not peer-reviewed version

Hydrothermal Co-Liquefaction of Sugarcane Bagasse and Residual Cooking Soybean Oil for Bio-Crude Production

Matheus Oliveira , Maria Pelisson , Fabiane Hamerski , Luís Ricardo Shigueyuki Kanda , Fernando Voll , Luiz Pereira Ramos , Marcos Lúcio Corazza *

Posted Date: 6 June 2024

doi: 10.20944/preprints202406.0341.v1

Keywords: bio-crude; hydrothermal co-liquefaction; ethanol; residual soybean oil; sugarcane bagasse

Preprints.org is a free multidiscipline platform providing preprint service that is dedicated to making early versions of research outputs permanently available and citable. Preprints posted at Preprints.org appear in Web of Science, Crossref, Google Scholar, Scilit, Europe PMC.

Copyright: This is an open access article distributed under the Creative Commons Attribution License which permits unrestricted use, distribution, and reproduction in any medium, provided the original work is properly cited.

Preprints.org (www.preprints.org) | NOT PEER-REVIEWED | Posted: 6 June 2024 doi:10.20944/preprints202406.0341.v1

Disclaimer/Publisher's Note: The statements, opinions, and data contained in all publications are solely those of the individual author(s) and contributor(s) and not of MDPI and/or the editor(s). MDPI and/or the editor(s) disclaim responsibility for any injury to people or property resulting from any ideas, methods, instructions, or products referred to in the content.

Article

Hydrothermal Co-Liquefaction of Sugarcane Bagasse and Residual Cooking Soybean Oil for Bio-Crude Production

Matheus Oliveira, Maria Pelisson, Fabiane Hamerski, Luís Kanda, Fernando Voll, Luiz Pereira Ramos and Marcos Lúcio Corazza *

Department of Chemical Engineering Department, Federal University of Paraná; Rua Coronel Francisco Heráclito dos Santos 100, Curitiba, PR 81531-980, Brazil; matheus.venancio@ufpr.br (M.O.); pelisson@ufpr.br (M.P.); fabianehamerski@ufpr.br (F.H.); kanda@ufpr.br (L.K.); fernando_voll@ufpr.br (F.V.); luiz.ramos@ufpr.br (L.P.R.); corazza@ufpr.br (M.L.C.)
* Correspondence: corazza@ufpr.br

Abstract: This study investigated different conditions for the hydrothermal co-liquefaction (co-HTL) of sugarcane bagasse and residual cooking soybean oil, with and without the presence of ethanol as a cosolvent to maximize the bio-crude yield. All co-HTL reactions were carried out in a 300 mL Parr® reactor at temperatures ranging from 200 to 300 °C. Bio-crude yields of around 95 wt.% were obtained at 300 °C using ethanol and water as solvents. The highest biochar yield (16.6 wt.%) was achieved when using only sugarcane bagasse as substrate, without the presence of soybean oil. Bio-crude samples obtained at higher temperatures (280 °C and 300 °C) using ethanol as a hydrogen donor presented higher contents of both free fatty acids and fatty acid ethyl esters. This work presents a promising process to produce high-quality bio-crude using an abundant feedstock (sugarcane bagasse) in the presence of a lipid source which could cause environmental problems if poorly handled.

Keywords: bio-crude; hydrothermal co-liquefaction; ethanol; residual soybean oil; sugarcane bagasse

1. Introduction

Biofuels and renewable energy sources have gained global attention due to the growing need for clean energy and fuels that can replace fossil fuels shortly [1]. Sugarcane bagasse stands out among the many possible options for new sources of energy, primarily in tropical countries. Around 151 million tons of sugarcane bagasse are produced worldwide annually [1] and part of this material is used to generate energy through its combustion in boilers and other cogeneration systems. However, better alternatives such as bio-crude, biofuels, synthetic oils, biochar, and hydrogenated fuels production can be explored for a more effective use of sugarcane bagasse [1,2]. Another widely generated material that does not have a proper destination is residual cooking and frying vegetable oils, which has the potential to be employed in various processes including biodiesel, green diesel, and biokerosene production [3]. The annual estimate for residual soybean oil is 16.54 million tons generated worldwide [4].

Thermal processes are a technically viable alternative for processing several biomass types and their scalability has been demonstrated for different feedstocks [5–7]. Among these processes, biomass hydrothermal liquefaction (HTL) is advantageous because it does not require a pre-drying process, meaning that using biomass with high moisture content is possible, even preferable. Furthermore, HTL bio-crudes can be produced from biomass at temperatures ranging from 250 to 400 °C in the presence or absence of co-solvents such as methanol, ethanol, glycerol, or even a mixture of solvents [8–10]. Table 1 summarizes studies that used different biomass types as feedstock and bio-crude yields, reaction parameters, and higher heating value (HHV) of products obtained.

© 2024 by the author(s). Distributed under a Creative Commons CC BY license.

Preprints.org (www.preprints.org) | NOT PEER-REVIEWED | Posted: 6 June 2024 doi:10.20944/preprints202406.0341.v1

Table 1. Literature review of biomasses used for bio-crude production.

Reference	Feedstock	Temperature (°C)	Pressure (MPa)	Bio-crude Yield (%)	Bio-crude HHV (MJ/Kg)
Vardon et al. (2011)	*Spirulina* sp.	300	10–12	32.6	33.2
	Swine manure	300	10–12	30.2	34.7
	Sludge	300	10–12	9.4	32
Cheng et al. (2017)	*Nannochloropsis salina* (CCMP1776)	310–350	-	18.1–27.5	27
Lavanya et al. (2016)	*Galdieria sulphuraria*	310–350	-	40–54.30	20.5
	Arthrospira platensis	250–350	18	30	38.65
	Tetraselmis sp.	250–350	18	29	35.58
López Barreiro et al. (2015)	*Almeriansis* sp.	-	-	42.6	-
	Gaditana sp.	-	-	50.8	-
Yan et al. (2019)	*Ulva prolifera* macroalgae	270, 290 and 310	4.3–7.0	26.7	-
Caporgno et al. (2016)	*Nannochloropsis oceana*	240–300	3.2–8.9	54.2	37.7
Kaur et al. (2019)	Castor beans	260, 280, and 300	-	15.8	14.43
Valdez et al. (2012)	*Nannochloropsis* sp.	250–400	-	46	-
Anastasakis et al. (2015)	*L. digitata*	350	-	17.6	32
	L. hyperbore	350	-	9.8	33
	L. saccharina	350	-	13	33.9
	A. esculenta	350	-	17.8	33.8
Anastasakis et al. (2018)	*Miscanthus* sp.	50–350	-	26	17.1
	Spirulina sp.	50–350	-	33	23.3
Ma et al. (2020)	*Ulva prolifera* macroalgae	260–300	4.3–7.0	32.2–34.8	
Zhang et al. (2018)	*Spirulina platensis*	400	40	22	17.26
Han et al. (2019)	*Tetraselmis* sp.	280-350	5–21	26–31	15.33
Tekin (2015)	Olive seeds	240-340	3.2–15	46.8	15.72

Preprints.org (www.preprints.org) | NOT PEER-REVIEWED | Posted: 6 June 2024 doi:10.20944/preprints202406.0341.v1

Vlaskin et al. (2018)	*Arthrospira platensis*	300	8.6	39.65–44.07	-
He et al. (2021)	Corn cob	300-360	10–20	22.2	32.6
	Cattle manure	300-360	10–20	19.3	35.5
Pedersen et al. (2015)	Poplar	380-400	-	38.05-52.26	-
Hu et al. (2018)	Rice husk	400	40	35.18	30.41-33.65
Posmanik et al. (2017)	Food waste	200-350	5–20	67	38
Baloch et al. (2021)	Sugarcane bagasse	280	-	38.42	34.61
Zhang et al. (2021)	Rice husk	250-350	1	88.77	39.07

Preprints.org (www.preprints.org) | NOT PEER-REVIEWED | Posted: 6 June 2024 doi:10.20944/preprints202406.0341.v1

Zhang et al. (2021) evaluated the effect of adding a lipid source such as a residual oil in HTL reactions using rice straw. Since two sources of biomasses were involved, the process was called hydrothermal co-liquefaction (co-HTL). While bio-crude yields of up to 50% have been achieved through HTL of biomass, adding a lipid agent has enhanced bio-crude yields by up to 80% [12–14]. Therefore, the main objective of this work was to investigate the co-HTL of a mixture of sugarcane bagasse and residual soybean oil, in the presence and absence of ethanol, at different process temperatures.

2. Materials and Methods

2.1. Materials

Residual soybean oil (RSO) was obtained from local residences. The RSO was first filtered using a domestic strainer to remove solid residues, followed by another filtration using filter paper to remove smaller solid impurities. Sugarcane bagasse (SCB) was supplied by Melhoramentos Norte do Paraná (Nova Londrina, PR, Brazil). Deionized water and ethanol (Neon, with 99.5% purity) were used as the reaction medium. Dichloromethane (DCM) (Neon, 99.5% purity) was used to recover the bio-crude after HTL. N_2 (White Martins, 99.9% purity) was used to create an inert atmosphere in the reaction media. All chemicals were used as received without further purification.

2.2. Experimental Procedures

Co-liquefaction was carried out in a Parr® (Moline, IL, USA) reactor coupled to a controller model 4848. The reactor consists of a 300 mL 316SS (stainless steel) vessel with an electric heating mantle and a mechanical agitation system. Reactions were carried out with SCB and SCB to RSO mass ratios of 1:3, 1:2, and 1:1 using a total biomass (RSO + SCB) to solvent mass ratio of 1:9 (Zhang et al., 2021). The reaction solvents were pure water and a mixture of water and ethanol (mass ratio of 1:1). Biomass and solvents were weighed on an analytical scale before being fed into the reactor.

After the biomass and solvents were fed into the reactor, N_2 gas was purged into the reactor for 3 min and, after that, the heating was started to initiate the reaction process. The reactor temperature setpoints (TSP) ranged from 250 to 300 °C. After reaching the temperature setpoint, the reaction was sustained for different holding times (tSP), which ranged from 10 to 120 min. Then, the system was cooled down to the ambient temperature, and around 60 mL DCM was added to clean the reactor walls and obtain a mixture containing bio-crude, solvents, and solids.

Vacuum filtration was performed using a Solab SL 60 vacuum pump (Piracicaba, SP, Brazil) to separate the solids from the liquid mixture. The filtrate was taken to a separating funnel to split the organic phase, in which light bio-crude is recovered, from the aqueous phase. The solid residue that remained in the filter paper was washed with ethanol to extract the heavy bio-crude phase from the solid phase. The "DCM + light bio-crude" and "ethanol + heavy bio-crude" mixtures were taken to a rotary evaporator to separate the bio-crudes from the solvents. The solid phase that remained on the filter paper was recovered, oven-dried at 105 °C for 24 h and weighed for mass yield calculations.

2.3. Bio-Crude and bio-char yield calculation

The bio-crude yield after HTL was calculated according to Equation (1),

$$Y_{bo}(\%) = \left(\frac{m_{bo}}{m_{scb} + m_{rso}}\right) \cdot 100 \quad (1)$$

where $Y_{bo}(\%)$ is the yield of bio-crude obtained, m_{bo} is the total bio-crude mass (heavy + light bio-crudes) obtained after rotary evaporation, m_{scb} is the mass of sugarcane bagasse added to the reactor, and m_{rso} is the total mass of residual frying oil added to the reactor.

The bio-char yield was calculated according to Equation (2),

$$Y_{bc}(\%) = \left(\frac{m_{bc}}{m_{scb}}\right) \cdot 100 \quad (2)$$

where $Y_{bc}(\%)$ is the bio-char yield and m_{bc} is the bio-char mass after drying.

2.4. Severity Index

The reactions performed in this study are non-isothermal because they involved both a heating

Preprints.org (www.preprints.org) | NOT PEER-REVIEWED | Posted: 6 June 2024 doi:10.20944/preprints202406.0341.v1

and a cooling ramp. To account for this non-isothermal behavior, the integral of the curve "temperature *vs* time" was calculated to determine a parameter known as the severity index (S_O). This value can be used as the kinetic (or pseudo-kinetic) factor for thermochemical reactions where a biomass fractionation exists in non-isothermal conditions (Carrasco et al., 1986; Bouchard et al., 1986; Heitz et al., 1986). In this study, S_O was calculated by integrating Equation (3) through the trapezoidal rule using the temperature profile measured during the reaction course,

$$S_O = log\left(\int_0^t exp\left[\frac{T(t) - Tb}{w}\right]dt\right) \quad (3)$$

where t is the reaction time in min; $T(t)$ is the temperature in °C as a function of time; Tb is a temperature reference value of 100 °C [36]; and w is a fixed parameter of 14.75, which corresponds to the activating energy of hemicellulose hydrolysis [36].

2.5. Bio-Crude and Bio-Char Characterization

For the analysis of mass loss and decomposition of the bio-crude and bio-char, a thermogravimetric analysis was performed using a PerkinElmer TGA 4000® analyzer. N_2 was applied as the carrier gas at temperatures ranging from 30 to 800 °C, with a heating rate of 10 °C/min. FT-IR analyses were performed to identify the main bio-crude and bio-char functional groups using a Bruker Alpha II® analyzer, with potassium bromide (KBr) disks as the crystalline surface. The higher heating value (HHV) was determined using a AC500 LECO® calorimeter according to ASTM D5468.

2.6. GC-FID Analysis

Free fatty acids, ethyl esters and tri, di and monoacylglycerols present in the bio-crude were quantified by gas chromatography in a Shimadzu GC-2010 equipped with an autosampler and a flame ionizing detector (FID). Analyses were performed in split mode (1:20) using a Select Biodiesel column (Agilent, 15 m x 0.32 mm, 0.10 µm) and helium as the carrier gas. The injector and detector temperatures were 380 °C and 400 °C, respectively. The oven temperature program started at 50 °C and reached 180 °C at 15 °C/min, then continued to 230 °C at 7 °C/min, and finally, to 380 °C at 10 °C/min, where it stayed for 6 min.

Initially, about 50 mg bio-crude was dissolved in 100 mL pyridine and 50 mL of the derivatizing agent N-methyl-N-(trimethylsilyl)trifluoroacetamide) was added. The mixture was vigorously shaken and maintained at 40 °C for 20 min. Subsequently, the derivatized sample was diluted in heptane to a final concentration of approximately 1 mg/mL and sent for GC-FID analysis. Quantifications were carried out by external calibration using linoleic acid, ethyl linoleate, and soybean oil as reference standards for the determination of total free fatty acids, ethyl esters, and triacylglycerols, respectively.

2.7. Phase Envelope of the Mixture (Water + Ethanol)

To have a better understanding of the solvent mixture dynamics during the non-isothermal process of batch co-HTL reactions, a phase envelope of the mixture (water + ethanol) was built. To do so, the Peng-Robinson equation of state was used with the quadratic mixture rule, in which the binary interaction parameters between water and ethanol were obtained from the literature [37].

Saturation lines were calculated following the algorithms proposed by Michelsen and Mollerup (2007), and implemented as described by Tavares et al. (2020). Critical lines for the mixture (water + ethanol) were calculated following the algorithm proposed by Michelsen and Mollerup (2007).

3. Results and Discussion

3.1. Bio-Crude and Bio-Char Yields

Table 2 presents both bio-crude and bio-char yields as a function of different reaction conditions and solvent systems. The heating and cooling profiles that were used to determine So for each reaction condition are shown in the Supplementary Material. The contents (as weight percentages) of fatty acid ethyl esters (FAEE), free fatty acids (FFA), and triacylglycerols (TAG) in the bio-crude were determined by GC-FID and are also given in Table 2.

Preprints.org (www.preprints.org) | NOT PEER-REVIEWED | Posted: 6 June 2024 doi:10.20944/preprints202406.0341.v1

Table 2. Results obtained at different co-HTL reaction conditions, with the (RSO+SCB) to solvents mass ratio fixed at 1:9.

Reaction ID	SCB:RSO Ratio	W:EtOH Ratio	TSP (°C)	tSP (min)	So	Y_{bo} (%)	FAEE (wt.%)	FFA (wt.%)	TAG (wt.%)	Y_{bc} (%)
1	1:3	1:0	275	10	6.55 ± 0.19	72.6 ± 1.6	NC	64.18	NC	0.4
2	1:3	1:0	250	10	5.86 ± 0.09	76.1 ± 0.6	NC	13.33	52.33	3.0 ± 1.1
3	1:3	1:0	300	10	7.59 ±0.06	66.6 ± 1.5	NC	60.72	NC	0.4 ± 0.2
4	1:3	1:1	250	10	5.94 ± 0.11	81.1 ± 4.5	NC	7.34	60.58	2.5 ± 2.1
5	1:3	1:1	275	10	6.61 ± 0.23	84.5 ± 3.5	10.60	31.65	14.53	2.8 ± 1.5
6	1:2	1:0	250	10	5.69 ± 0.23	76.0 ± 0.0	NC	9.21	55.24	4.3 ± 1.0
7	1:2	1:0	275	10	6.54 ± 0.04	71.0 ± 4.8	2.74	37.68	NC	0.9 ± 0.1
8	1:1	1:0	275	10	6.48 ± 0.01	58.1 ± 2.7	2.17	39.03	NC	2.6 ± 0.8
9	1:2	1:1	275	10	6.67 ± 0.17	73.9 ± 5.4	5.63	21.93	21.63	3.5 ± 2.5
10	1:1	1:1	275	10	6.78 ± 0.03	66.6 ± 2.1	13.57	36.51	NC	2.6 ± 1.8
11	1:0	1:0	275	10	6.50 ± 0.02	21.3 ± 0.3	NA	NA	NA	16.6 ± 3.2
12	1:0	1:1	275	10	6.60 ± 0.13	30.5 ± 6.0	NA	NA	NA	11.6 ± 3.5
13	1:2	1:0	300	10	7.33 ± 0.01	70.7 ± 7.2	NC	54.82	NC	0.4 ± 0.2
14	1:3	1:1	280	10	7.24 ± 0.20	91.5 ± 1.0	39.83	32.35	NC	0.4 ± 0.1
15	1:3	1:1	300	50	7.75	95.1	35.36	34.95	NC	0.0
16	1:3	1:1	250	60	6.28	88.8	7.75	4.85	NC	3.2
17	1:3	1:1	275	60	7.11	95.0	27.02	15.74	NC	0.4
18	1:1	1:1	290	120	7.87	80.2	38.82	30.69	NC	0.9
19	1:2	1:1	300	120	8.08	89.0	43.98	34.26	NC	0.0
20	1:3	1:1	200	10	2	0.0	NC	NC	55.52	0.0

SCB:RSO = SCB to RSO mass ratio; W:EtOH = water to ethanol mass ratio; (SCB+RSO):S = SCB plus RSO mass ratio in relation to solvents (water + ethanol); TSP (°C) = setpoint temperature for the reaction; tSP (min) = holding time at the setpoint temperature; Y_{bo} (%) = bio-crude yield; Y_{bc} (%) = bio-char yield; FAEE = fatty acid ethyl esters; FFA = free fatty acids; and TAG = triacylglycerols; NA = samples not analyzed by GC-FID; NC = not detected..

Table 2 demonstrated that variables such as temperature, SCB to RSO mass ratio, and reaction time have a direct influence on bio-crude yields, and this will be discussed in detail in the upcoming sections. The highest biochar yields were obtained when RSO was absent in the reaction mixture, indicating that biochar production is connected to the amount of sugarcane bagasse proportionally available for thermal conversion. A 16.6% bio-char was obtained in reaction 11, when only water was used as solvent, whereas in reaction 12, the replacement of water by the water and ethanol mixture decreased the biochar yield to 11.6%.

3.2. Effect of SCB to RSO Mass Ratio

Reactions were performed in the presence of water or a water and ethanol mixture at a mass ratio of 1:1. Figure 1 presents the effect of SCB to RSO mass ratio on bio-crude yields at the same setpoint temperature (275 °C), holding time at setpoint temperature (10 min) and solvents to biomass mass ratio (9:1). Regardless of the solvent used, higher RSO additions led to higher bio-crude yields. By contrast, reactions performed without RSO (reactions 11 and 12) resulted in two out of the three lowest bio-crude yields (21.3% and 30.5%, respectively). When the same conditions were applied to reactions with SCB to RSO mass ratio of 1:1 (reactions 8 and 10), bio-crude yields increased to 58.1% and 66.6%, respectively. Forero et al. (2022) performed HTL reactions using SCB in the presence of different solvents without RSO addition. The maximum bio-crude yield was 66.1%, which confirms the positive impact of RSO on reaction performance.

Preprints.org (www.preprints.org) | NOT PEER-REVIEWED | Posted: 6 June 2024 doi:10.20944/preprints202406.0341.v1

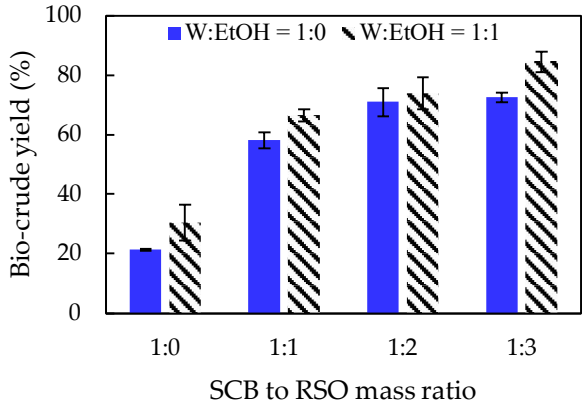

Figure 1. Effect of SCB to RSO mass ratio on bio-crude yield. Reaction conditions kept constant were: set point temperature of 275 ºC, holding time of 10 min, and solvent (W+EtOH) to biomass (SCB+RSO) mass ratio of 9:1. SCB = sugarcane bagasse; RSO = residual soybean oil; W = water; EtOH = ethanol; W:EtOH = water to ethanol mass ratio.

When pure water is used as a solvent, hydrolysis of triacylglycerols takes place forming free fatty acids plus diacylglycerols and monoacylglycerols. However, when the solvent is a water and ethanol mixture, other reactions occur along with hydrolysis, such as transesterification of triacylglycerols and esterification of free fatty acids, producing fatty acid ethyl esters, diacylglycerols, monoacylglycerols, and glycerol. Since acylglycerols, free fatty acids, and fatty acid ethyl esters have low polarity, they remain in the organic phase, enhancing the bio-crude yield.

The highest yield of 84.5% was obtained for an SCB to RSO mass ratio of 1:3 using ethanol and water as solvents (reaction 5), indicating that this is the most suitable solvent for the co-HTL system. When pure water was used as solvent, the highest yield (72.6%, reaction 1) was also obtained for a SCB to RSO mass ratio of 1:3. Analyses the bio-crude compositions by GC-FID (see Table 2) revealed that the FFA content was much higher for reactions performed with pure water, while the FAEE content was higher when the mixture (water + ethanol) was used.

The presence of ethanol during co-HTCL reactions may also prevent the occurrence of undesired reactions, such as polymerization, and contributes to a lower viscosity and higher quality of the bio-crude, minimizing degradation, viscosity, instability through time and coke formation [40].

3.3. Effect of Temperature on Bio-Crude Yield

The effect of temperature on bio-crude yields can be observed in Figure 2 for reactions performed with SCB to RSO mass ratios of 1:2 and 1:3 and water to ethanol mass ratios of 1:0 (Figure 2.a) and 1:1 (Figure 2.b). Other reaction conditions involved a holding time of 10 min and a solvents to biomasses mass ratio of 9:1.

The reactions using pure water (Figure 2.a) showed a decrease in bio-crude yields as the temperature increased for both SCB to RSO mass ratios (1:2 and 1:3). Therefore, the highest yields of 76.1% (reaction 2) and 76.0% (reaction 6) were obtained at 250 °C for SCB:RSO ratios of 1:3 and 1:2, respectively. For reactions using pure water at higher temperatures, some compounds present in the SCB might have dissolved and were not recovered in the organic phase (DCM-rich phase), justifying the observed decrease in bio-crude yields [41].

Preprints.org (www.preprints.org) | NOT PEER-REVIEWED | Posted: 6 June 2024 doi:10.20944/preprints202406.0341.v1

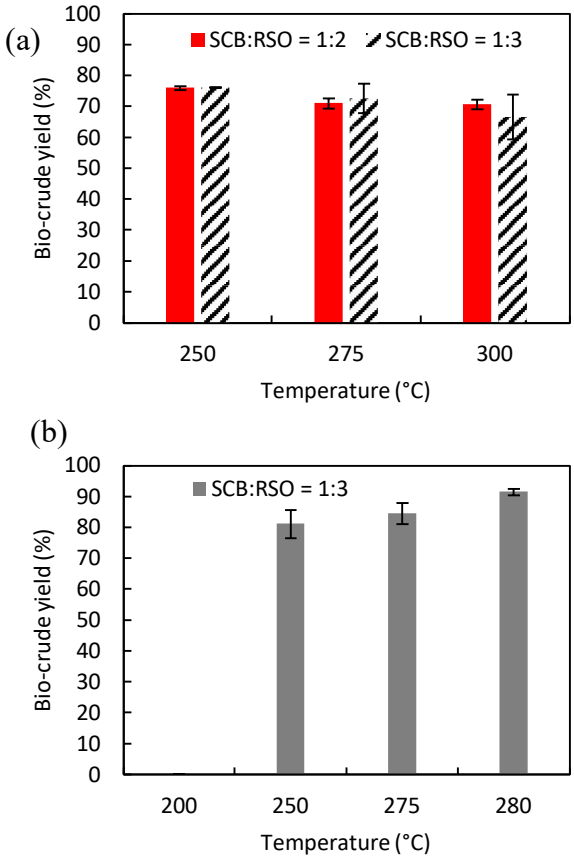

Figure 2. Effect of temperature in the bio-crude yield for (**a**) W:EtOH = 1:0, and (**b**) W:EtOH = 1:1. Reaction conditions kept constant were: holding time of 10 min and solvent (W+EtOH) to biomass (SCB+RSO) mass ratio of 9:1. SCB = sugarcane bagasse; RSO = residual soybean oil; W = water; EtOH = ethanol; W:EtOH = water to ethanol mass ratio.

Figure 2.b shows that, for reactions carried out using the solvent mixture (water + ethanol), higher bio-crude yields were obtained at higher temperatures (*e.g.*, 91.5% at 280 °C in reaction 14). For all temperatures studied, the bio-crude yield was higher when the solvent used was the mixture of ethanol and water, indicating once again that the use of such a mixture may be more interesting for co-HTL reactions rather than pure water.

It is worth mentioning that both bio-crude and bio-char yields after reaction 20 were zero because the resulting solids resembled untreated SCB. This also indicates that the reaction temperature was too low for HTL which, according to our data, required a minimum setpoint temperature of 250 °C.

3.4. Effect of Severity Index in Bio-Crude Yield

The combined effect of temperature and reaction time on bio-crude yield was also studied through the severity index. Reactions with different holding times at the same temperature were performed to study the effect of reaction time on bio-crude yield. The severity indices were obtained from the heating and cooling profiles presented in the Supplementary Material, using the methodology described in Section 2.4. Figures 3.a and 3.b show severity indices that were calculated for reactions using water and a as solvents, respectively.

Figure 3.a shows that high severity indices led to low bio-crude yields, meaning that they are inversely proportional. By contrast, when the water and ethanol mixture was used as solvent (Figure 3.b), this trend was reversed, with severity indices and bio-crude yields becoming directly proportional.

Preprints.org (www.preprints.org) | NOT PEER-REVIEWED | Posted: 6 June 2024 doi:10.20944/preprints202406.0341.v1

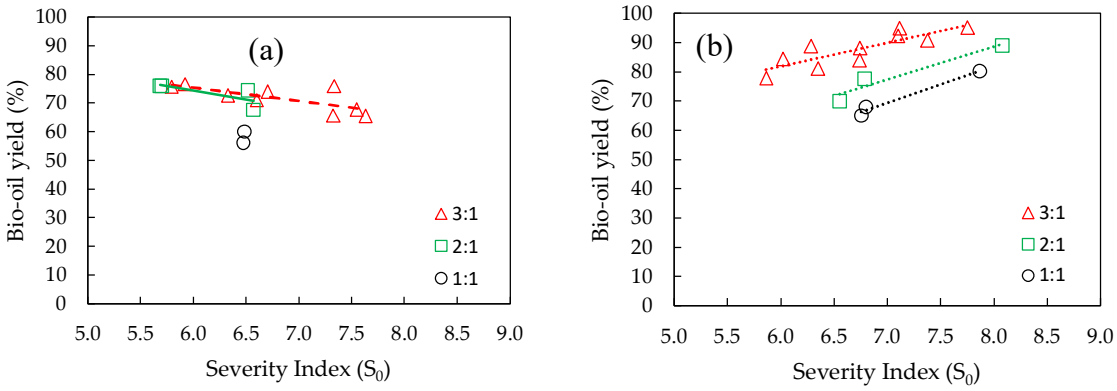

Figure 3. Bio-crude yield as a function of severity index in co-HTL reactions using (**a**) water as solvent, and (**b**) water and ethanol (mass ratio of 1:1). Solvent (W+EtOH) to biomass (SCB+RSO) mass ratio was kept constant at 9:1 for all reactions. SCB = sugarcane bagasse; RSO = residual soybean oil; W = water; EtOH = ethanol.

Some reactions (reactions 2, 4, 6, and 20) resulted in a bio-crude with higher TAG concentrations (above 50 wt.%) and few to no FAEE because their severity indices were relatively low (below 5.94), indicating that the reaction process was inefficient. Reactions 2 and 6 were performed at 250 °C using pure water as solvent, while reactions 4 and 20 were carried out at 200 °C and 250 °C, respectively, using the water and ethanol mixture as solvent.

Other reactions (reactions 14, 15, 17, and 19), performed with the water and ethanol mixture as solvent, presented higher FAEE contents (above 27 wt.%) at temperatures above 275 °C. These samples were generated at the highest severity indices (above 7.11), indicating that if the combination of setpoint temperature and time at the setpoint temperature is appropriate, high bio-crude yields and high FAEE contents in bio-crude can be achieved.

To summarize the severity index analysis, Figure 4 presents the bio-crude yields that were obtained at the highest severity indices (reactions 15, 18, and 19) used in this study. These reactions were performed using the water and ethanol mixture as solvent and a solvents to biomass (SCB+RSO) mass ratio of 9:1. Among these three reaction conditions, it was not possible to infer a monotonic behavior: the highest bio-crude yield was obtained for the lowest severity index, but the highest severity index did not result in the lowest bio-crude yield. The fact that these reactions were not performed at the same temperature should not be an issue because the severity index adjusts the variables temperature and reaction time. On the other hand, it was evident that the SCB to RSO mass ratio has an impact on bio-crude yield and must be considered.

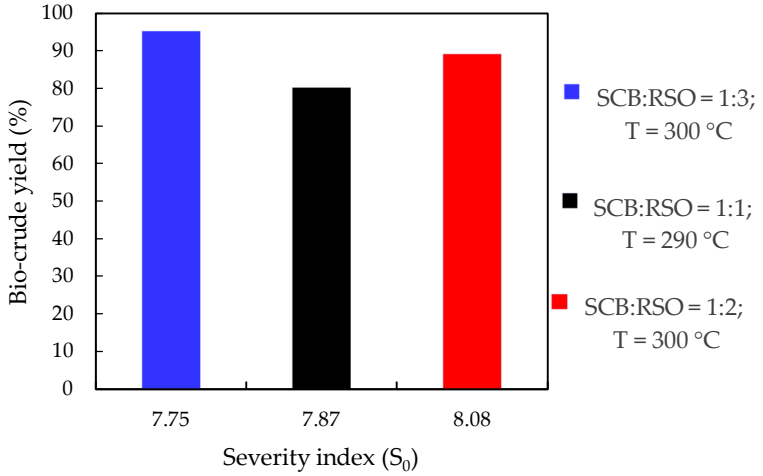

Preprints.org (www.preprints.org) | NOT PEER-REVIEWED | Posted: 6 June 2024 doi:10.20944/preprints202406.0341.v1

Figure 4. Bio-crude yield as a function of severity index in co-HTL reactions using a mixture (ethanol + water) as solvent and solvent (W+EtOH) to biomass (SCB+RSO) mass ratio of 9:1. SCB = sugarcane bagasse; RSO = residual soybean oil; W = water; EtOH = ethanol. Note: x-axis is not in scale.

3.5. TGA Analysis of Bio-Crude and Bio-Char

Figures 5.a and 5.b show the TGA profiles for bio-crude samples produced with pure water and with the water and ethanol mixture, respectively, with a solvents to biomass (SCB+RSO) mass ratio of 9:1.

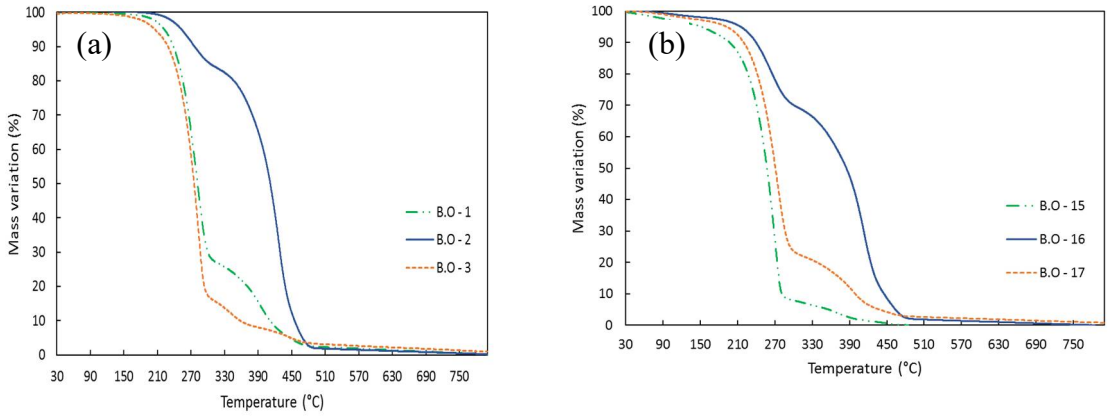

Figure 5. TGA curves of bio-crudes produced at different temperatures (**a**) with pure water and (**b**) with a mixture (water + ethanol). B.O-2 and B.O-16 are bio-crudes produced at 250 °C; B.O-1 and B.O-17 are bio-crudes produced at 275 °C; B.O-3 and B.O-15 are bio-crudes produced at 300 °C.

Figures 5.a and 5.b revealed similarities among the TGA profiles of all bio-crude samples: the first mass loss event has onset temperatures of 220-240 °C, the second mass loss event has onset temperatures 360-390 °C and the total mass loss reached almost 100% after 450-500 °C. On the other hand, Figure 5.b showed small mass losses at temperatures below 100 °C, demonstrating that solvents still might be present in bio-crudes obtained using the water and ethanol mixture.

A similar mass loss profiles was also observed for samples obtained at the same temperatures, whether ethanol was present in the reaction media or not (Figures 5.a and 5.b). In this sense, bio-crude samples obtained at 250 °C (reactions 2 and 16) and at 275 °C (reactions 1 and 17) had two well-defined mass loss events, while for bio-crude samples obtained at 300 °C (reactions 3 and 15), only the first mass loss was well-defined. On the other hand, the use of pure water or water plus ethanol led to different bio-crude compositions (Table 2), which may partly explain the differences in mass loss among samples obtained at the same reaction temperature.

The first mass loss event can be attributed mainly to the evaporation of free fatty acids and fatty acid ethyl esters [42,43], while the second mass loss event can be primarily attributed to the evaporation of acylglycerols [44]. It is also important to mention that these bio-crude samples contained light and heavy fractions (the former obtained after separation of the liquid phase using DCM and the latter obtained by extraction of the solid phase with ethanol). Heavy bio-crudes tend to present TGA profiles similar to those of petroleum-based phenolic resins and bio-resins produced by direct liquefaction of lignocellulosic materials [45,46].

Figure 6 shows the TGA for bio-chars produced with pure water and a water and ethanol mixture at different temperatures. There was a great difference in mass loss profiles when different solvents were used. Biochar sample 2 presented a sharp mass loss starting around 350 °C, which led to a final mass loss close to 60%, indicating bad thermal stability. It is important to mention that, at 250 °C, the reaction was possibly incomplete because the mass loss obtained by TGA was very similar to the results of other authors for SCB [1,47]. For bio-char samples 14 and 18, the mass loss was minimal, indicating a good thermal stability [48].

Preprints.org (www.preprints.org) | NOT PEER-REVIEWED | Posted: 6 June 2024 doi:10.20944/preprints202406.0341.v1

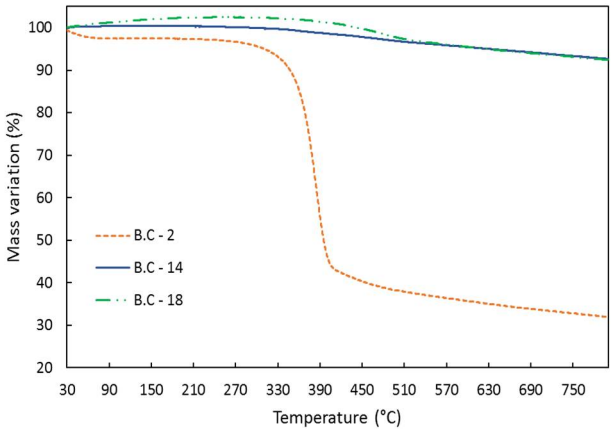

Figure 6. TGA Analysis for bio-char samples produced with pure water and with a mixture (water + ethanol). B.C-2 is the bio-char produced at 250 °C using water; B.C-14 and B.C-18 are the bio-chars produced at 280 °C and 290 °C using water plus ethanol, respectively.

3.6. FTIR Analysis of Bio-Crude and Bio-Char

The FTIR spectra of bio-crudes obtained using pure water and water plus ethanol are presented in Figures 7.a and 7.b, respectively, while that for bio-char samples are given in Figure 8. Samples were chosen to compare products derived from different reactional conditions.

In Figures 7.a and 7.b, bands at 1000-1325 cm^{-1} are attributed to the C–OH, C–O–C, and C–O stretching, and at 1325-1450 cm^{-1} to the C–O stretching of glycerol moieties present in acylglycerols. Bands at 1600-1900 cm^{-1} correspond to the C=O stretching of carbonylated compounds, indicating that the bio-crudes may have aldehydes, carboxylic acids, esters, and ketones in their composition. Bands ranging from 1450-1600 cm^{-1}, related to C=C stretching, indicate the presence of alkyl aromatics and aliphatics in bio-crudes. Bands between 2750-3100 cm^{-1} are related to the C–H stretching of CH, CH_2, and CH_3, while the broad band at 3250-3700 cm^{-1} is related to the O–H stretching of hydroxylated functional groups such as phenols and alcohols, but it may also be due to the presence moisture content [1,49].

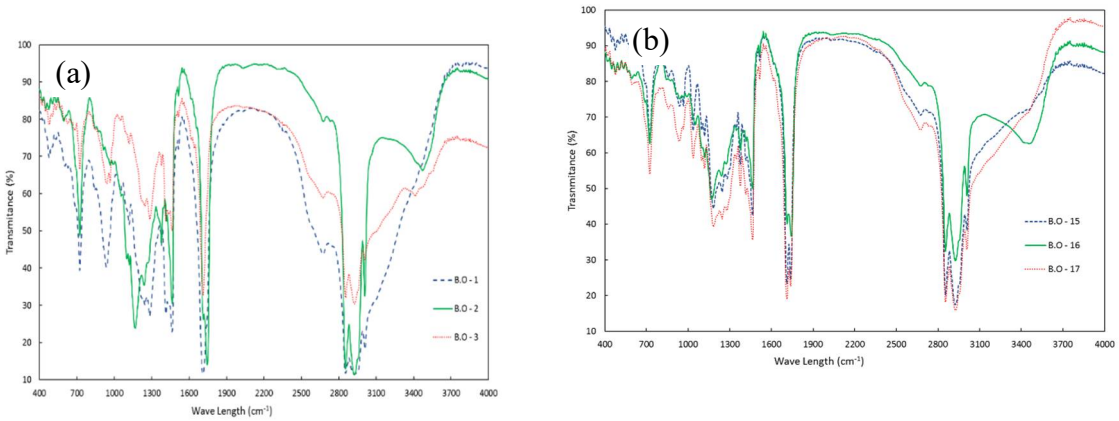

Figure 7. FTIR analysis for bio-crude samples produced (a) with pure water and (b) with the mixture (water + ethanol) as solvent. B.O-2 and B.O-16 are bio-crudes produced at 250 °C; B.O-1 and B.O-17 are bio-crudes produced at 275 °C; B.O-3 and B.O-15 are bio-crude produced at 300 °C.

Samples 1 and 3 presented very similar FTIR spectra, while sample 2 presented some differences, especially in the 1100-1500 cm^{-1} wavenumber range. According to Table 2, the main difference between samples 1 and 3 and sample 2 is the TAG content, which is confirmed by the differences observed by FT-IR in Figure 7.a. Likewise, Figure 7.b show similar spectra for samples 15, 16 and 17, indicating similar compositions as already described in Table 2.

Preprints.org (www.preprints.org) | NOT PEER-REVIEWED | Posted: 6 June 2024 doi:10.20944/preprints202406.0341.v1

The FTIR spectra of bio-char samples 15 and 18 were also very similar, while sample 2, obtained at a lower temperature, presented a spectrum more closely related to untreated SCB (Figure 8). This confirms once more that 250 °C was too low for HTL.

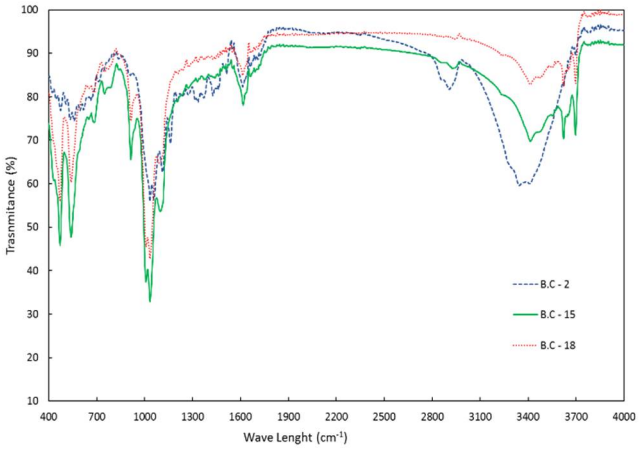

Figure 8. FTIR analysis for bio-char samples produced with different solvents and bagasse to residual oil mass ratios. B.C-2 is the bio-char produced at 250 °C using water; B.C-18 and B.C-15 are the bio-chars produced at 290 °C and 300 °C using water plus ethanol.

3.7. HHV Analysis of Bio-Crude and Bio-Char Samples

Table 3 presents the higher heating value (HHV) of bio-crudes and bio-chars, as well as the SCB and RSO used in co-HTL. In general, HHV values were above 37 MJ/kg and are below 16 MJ/kg for bio-crudes and bio-chars, respectively. Among the bio-char samples, the lowest HHV value (8.3 MJ/kg) was related to reaction 14, which provided high contents of both FAEE and FFA, indicating a considerable conversion of biomasses, especially SCB, into bio-crude. The HHV value of the bio-crude is almost 4 times higher than that of SCB.

Values of HHV obtained in the present study are in agreement with similar studies presented in the literature. Forero et al. (2022) produced bio-crude from SCB in HTL reactions using water, mixture of water and ethanol, and mixture of water and glycerol, reaching HHV values from 26.58 to 34.57 MJ/kg. Zhang et al. (2021) used rice husks in the presence of residual frying oil in co-HTL reactions having water and glycerol as solvents and the bio-crudes obtained presented HHV values of ranging from 28.4 to 39.07 MJ/kg.

Table 3. HHV values obtained for bio-crude, bio-char, SCB, and RSO. B.O-X are different bio-crudes and B.C-X are different bio-chars, where X indicates the reaction condition presented in Table 2; SCB = sugarcane bagasse; RSO = residual soybean oil.

Sample	HHV (MJ/kg)
B.O - 2	38.81
B.O - 15	38.41
B.O - 16	37.78
B.O - 17	37.82
B.O - 18	38.14
B.O - 19	38.46
B.C - 14	8.30
B.C - 16	16.04
SCB	10.38
RSO	39.34

3.8. Analysis of the Reaction Projection in the Phase Envelope of the Mixture (Water + Ethanol)

The phase envelopes for pure water, pure ethanol, and a 1:1 (mass ratio) binary mixture (water + ethanol), which was used in the co-HTL reactions, are presented in the Supplementary Material.

Preprints.org (www.preprints.org) | NOT PEER-REVIEWED | Posted: 6 June 2024 doi:10.20944/preprints202406.0341.v1

From the phase envelopes, it is possible to observe that the temperature-pressure profiles of the reactions correspond to the line of pure water vapor when using water as the solvent and are consistent with the liquid-vapor envelope for the binary mixture (water + ethanol) when using such mixture in the reactions. In a general manner, the reactions performed in this work were projected in the saturation region of the solvents involved in the process. However, for reaction 15, both temperature and pressure reached the supercritical region of the (water + ethanol) mixture, and this may explain why this reaction provided a higher bio-crude yield.

The Supplementary Material also presents a projection of temperature and pressure curves overlapping the phase envelope of the mixture (water + ethanol), which provides a view of the non-isothermal path of the reactions, *i. e.*, heating and cooling of the closed-vessel reactor, in which the heating and cooling profiles follow the bubble point and dew point lines, respectively. This indicates that the system does not suffer from overheating and reiterates that such a system must be monitored using a non-isothermal parameter, such as the severity index.

5. Conclusions

The present work contributes to the study of co-HTL reactions with an abundant biomass feedstock (sugarcane bagasse, SCB) in the presence of a renewable lipid source that could cause environmental problems if poorly disposed. The presence of residual soybean oil (RSO) in the co-HTL reactions had a positive impact on bio-crude yield. Furthermore, the mixture (water + ethanol) was more advantageous for the obtainment of higher bio-crude yields in HTL and co-HTL reactions.

The severity index (S_0), a parameter that combines the effects of temperature and reaction time, was used in this work to evaluate the non-isothermal conditions of the reaction system. For co-HTL reactions performed with the mixture (water + ethanol) as solvent, higher severity indices generally resulted in higher bio-crude yields, given that appropriate amounts of RSO were used. An analysis of the (water + ethanol) phase envelope indicated that the operation of co-HTL reactions above or close to the critical point of the solvent mixture might be necessary to obtain higher bio-crude yields.

Characterization of bio-crude samples, which included TGA, FTIR, HHV, and GC-FID, indicated that the samples presented high HHV, a favorable mass loss profile, and the presence of bonds and functionals groups that are typical of bio-crudes in general. The co-HTL of SCB in the presence of RSO, along with the use of a binary solvent system and the ancillary separation methods, was a promising procedure to produce bio-crude in high yields and high quality.

Supplementary Materials: The following supporting information can be downloaded at the website of this paper posted on Preprints.org, Figure S1. Heating and pressure profiles of a 10 min reaction course using the water and ethanol mixture as solvents; Figure S.2. Heating and pressure profile of a 10 min reaction course using water as solvent; Figure S.3. Heating and pressure profile of 50 and 60 min reaction courses using water as solvent; Figure S.4. Heating and pressure profile of a 120 min reaction course using water as solvent; Figure S.5. Phase envelope for the reactional system of interest: lines represent the saturation line for the pure components water and ethanol. Open symbols represent the maximum coordinates of temperature and pressure that were reached during the experiments with pure water (blue triangles) and with water and ethanol mixture (black squares). The crosses represent the critical points of pure components (blue cross: water, and red cross: ethanol). The dotted green line represents the critical line of the water and ethanol mixture, calculated with EoS-PR; Figure S6. Phase envelope for water and ethanol system with projection of the heating and cooling curves of the reactional system.

Author Contributions: Conceptualization, M. O. and M. L. C.; methodology, M. O., M. P., F. H., and M. C.; formal analysis, M. O. and F. H.; investigation, M. O., M. P. and F. H.; resources, M. L. C., data curation, M. O., F. V., L. K., L. P. R. and M. L. C.; writing—original draft preparation, M. O., L. K. and F. V.; writing—review and editing, L. P. R. and M. L. C.; supervision, M. L. C.; project administration, M. L. C.; funding acquisition, M. L. C. and L. P. R. All authors have read and agreed to the published version of the manuscript.

Funding: This research was funded by Fundação Araucária - NAPI -HCR, grant number 02/2021 and CNPq, grant number 405732/2022-8. Check carefully that the details given are accurate and use the standard spelling of funding agency names at https://search.crossref.org/funding. Any errors may affect your future funding.

Data Availability Statement: Data are contained within the article.

Preprints.org (www.preprints.org) | NOT PEER-REVIEWED | Posted: 6 June 2024 doi:10.20944/preprints202406.0341.v1

Acknowledgments: The authors would like to acknowledge Fundacao Araucaria and NAPI for the support of this project. M. L. C. thanks CNPq for the financial support and the scholarship Proc. Num. 310038/2020-0).

Conflicts of Interest: The authors declare no conflicts of interest.

References

1. Baloch, H.A.; Nizamuddin, S.; Siddiqui, M.T.H.; Mubarak, N.M.; Dumbre, D.K.; Srinivasan, M.P.; Griffin, G.J. Sub-Supercritical Liquefaction of Sugarcane Bagasse for Production of Bio-Oil and Char: Effect of Two Solvents. *J Environ Chem Eng* **2018**, *6*, 6589–6601, doi:10.1016/j.jece.2018.10.017.
2. Forero, J.A.J.; Tran, T.H.T.; Tana, T.; Baker, A.; Beltramini, J.; Doherty, W.O.S.; Moghaddam, L. Hydrothermal Liquefaction of Sugarcane Bagasse to Bio-Oils: Effect of Liquefaction Solvents on Bio-Oil Stability. *Fuel* **2022**, *312*, doi:10.1016/j.fuel.2021.122793.
3. Almeida, L.; Corazza, M.L.; Sassaki, G.L.; Voll, F.A.P. Experimental Study and Kinetic Modeling of Waste Frying Soybean Oil Hydrolysis in Subcritical Water. *Reaction Kinetics, Mechanisms and Catalysis* **2017**, *121*, 439–452, doi:10.1007/s11144-017-1175-1.
4. Irsyad, M.; Amrizal; Harmen; Amrul; Susila Es, M.D.; Diva Putra, A.R. Experimental Study of the Thermal Properties of Waste Cooking Oil Applied as Thermal Energy Storage. *Results in Engineering* **2023**, *18*, doi:10.1016/j.rineng.2023.101080.
5. Pedersen, T.H.; Jasiunas, L.; Casamassima, L.; Singh, S.; Jensen, T.; Rosendahl, L.A. Synergetic Hydrothermal Co-Liquefaction of Crude Glycerol and Aspen Wood. *Energy Convers Manag* **2015**, *106*, 886–891, doi:10.1016/j.enconman.2015.10.017.
6. He, S.; Wang, J.; Cheng, Z.; Dong, H.; Yan, B.; Chen, G. Synergetic Effect and Primary Reaction Network of Corn Cob and Cattle Manure in Single and Mixed Hydrothermal Liquefaction. *J Anal Appl Pyrolysis* **2021**, *155*, doi:10.1016/j.jaap.2021.105076.
7. Ranganathan, P.; Savithri, S. Techno-Economic Analysis of Microalgae-Based Liquid Fuels Production from Wastewater via Hydrothermal Liquefaction and Hydroprocessing. *Bioresour Technol* **2019**, *284*, 256–265, doi:10.1016/j.biortech.2019.03.087.
8. Zhang, C.; Han, L.; Yan, M.; Xia, J.; Rong, N.; Baloch, H.A.; Guo, H.; Wu, P.; Xu, G.; Ma, K. Hydrothermal Co-Liquefaction of Rice Straw and Waste Cooking-Oil Model Compound for Bio-Crude Production. *J Anal Appl Pyrolysis* **2021**, *160*, doi:10.1016/j.jaap.2021.105360.
9. Pedersen, T.H.; Jasiunas, L.; Casamassima, L.; Singh, S.; Jensen, T.; Rosendahl, L.A. Synergetic Hydrothermal Co-Liquefaction of Crude Glycerol and Aspen Wood. *Energy Convers Manag* **2015**, *106*, 886–891, doi:10.1016/j.enconman.2015.10.017.
10. Mishra, R.K.; Kumar, V.; Kumar, P.; Mohanty, K. Hydrothermal Liquefaction of Biomass for Bio-Crude Production: A Review on Feedstocks, Chemical Compositions, Operating Parameters, Reaction Kinetics, Techno-Economic Study, and Life Cycle Assessment. *Fuel* **2022**, *316*, 123377, doi:https://doi.org/10.1016/j.fuel.2022.123377.
11. Zhang, C.; Han, L.; Yan, M.; Xia, J.; Rong, N.; Baloch, H.A.; Guo, H.; Wu, P.; Xu, G.; Ma, K. Hydrothermal Co-Liquefaction of Rice Straw and Waste Cooking-Oil Model Compound for Bio-Crude Production. *J Anal Appl Pyrolysis* **2021**, *160*, doi:10.1016/j.jaap.2021.105360.
12. Teri, G.; Luo, L.; Savage, P.E. Hydrothermal Treatment of Protein, Polysaccharide, and Lipids Alone and in Mixtures. *Energy and Fuels* **2014**, *28*, 7501–7509, doi:10.1021/ef501760d.
13. He, S.; Wang, J.; Cheng, Z.; Dong, H.; Yan, B.; Chen, G. Synergetic Effect and Primary Reaction Network of Corn Cob and Cattle Manure in Single and Mixed Hydrothermal Liquefaction. *J Anal Appl Pyrolysis* **2021**, *155*, doi:10.1016/j.jaap.2021.105076.
14. Leng, L.; Li, J.; Yuan, X.; Li, J.; Han, P.; Hong, Y.; Wei, F.; Zhou, W. Beneficial Synergistic Effect on Bio-Oil Production from Co-Liquefaction of Sewage Sludge and Lignocellulosic Biomass. *Bioresour Technol* **2018**, *251*, 49–56, doi:10.1016/j.biortech.2017.12.018.
15. Vardon, D.R.; Sharma, B.K.; Scott, J.; Yu, G.; Wang, Z.; Schideman, L.; Zhang, Y.; Strathmann, T.J. Chemical Properties of Biocrude Oil from the Hydrothermal Liquefaction of Spirulina Algae, Swine Manure, and Digested Anaerobic Sludge. *Bioresour Technol* **2011**, *102*, 8295–8303, doi:10.1016/j.biortech.2011.06.041.
16. Cheng, F.; Cui, Z.; Chen, L.; Jarvis, J.; Paz, N.; Schaub, T.; Nirmalakhandan, N.; Brewer, C.E. Hydrothermal Liquefaction of High- and Low-Lipid Algae: Bio-Crude Oil Chemistry. *Appl Energy* **2017**, *206*, 278–292, doi:10.1016/j.apenergy.2017.08.105.
17. Lavanya, M.; Meenakshisundaram, A.; Renganathan, S.; Chinnasamy, S.; Lewis, D.M.; Nallasivam, J.; Bhaskar, S. Hydrothermal Liquefaction of Freshwater and Marine Algal Biomass: A Novel Approach to Produce Distillate Fuel Fractions through Blending and Co-Processing of Biocrude with Petrocrude. *Bioresour Technol* **2016**, *203*, 228–235, doi:10.1016/j.biortech.2015.12.013.
18. López Barreiro, D.; Riede, S.; Hornung, U.; Kruse, A.; Prins, W. Hydrothermal Liquefaction of Microalgae: Effect on the Product Yields of the Addition of an Organic Solvent to Separate the Aqueous Phase and the Biocrude Oil. *Algal Res* **2015**, *12*, 206–212, doi:10.1016/j.algal.2015.08.025.

Preprints.org (www.preprints.org) | NOT PEER-REVIEWED | Posted: 6 June 2024 doi:10.20944/preprints202406.0341.v1

19. Yan, L.; Wang, Y.; Li, J.; Zhang, Y.; Ma, L.; Fu, F.; Chen, B.; Liu, H. Hydrothermal Liquefaction of Ulva Prolifera Macroalgae and the Influence of Base Catalysts on Products. *Bioresour Technol* **2019**, *292*, doi:10.1016/j.biortech.2019.03.125.
20. Caporgno, M.P.; Pruvost, J.; Legrand, J.; Lepine, O.; Tazerout, M.; Bengoa, C. Hydrothermal Liquefaction of Nannochloropsis Oceanica in Different Solvents. *Bioresour Technol* **2016**, *214*, 404–410, doi:10.1016/j.biortech.2016.04.123.
21. Kaur, R.; Gera, P.; Jha, M.K.; Bhaskar, T. Reaction Parameters Effect on Hydrothermal Liquefaction of Castor (Ricinus Communis)Residue for Energy and Valuable Hydrocarbons Recovery. *Renew Energy* **2019**, *141*, 1026–1041, doi:10.1016/j.renene.2019.04.064.
22. Valdez, P.J.; Nelson, M.C.; Wang, H.Y.; Lin, X.N.; Savage, P.E. Hydrothermal Liquefaction of Nannochloropsis Sp.: Systematic Study of Process Variables and Analysis of the Product Fractions. *Biomass Bioenergy* **2012**, *46*, 317–331, doi:10.1016/j.biombioe.2012.08.009.
23. Anastasakis, K.; Ross, A.B. Hydrothermal Liquefaction of Four Brown Macro-Algae Commonly Found on the UK Coasts: An Energetic Analysis of the Process and Comparison with Bio-Chemical Conversion Methods. *Fuel* **2015**, *139*, 546–553, doi:10.1016/j.fuel.2014.09.006.
24. Anastasakis, K.; Biller, P.; Madsen, R.B.; Glasius, M.; Johannsen, I. Continuous Hydrothermal Liquefaction of Biomass in a Novel Pilot Plant with Heat Recovery and Hydraulic Oscillation. *Energies (Basel)* **2018**, *11*, doi:10.3390/en11102695.
25. Ma, C.; Geng, J.; Zhang, D.; Ning, X. Hydrothermal Liquefaction of Macroalgae: Influence of Zeolites Based Catalyst on Products. *Journal of the Energy Institute* **2020**, *93*, 581–590, doi:10.1016/j.joei.2019.06.007.
26. Zhang, B.; Feng, H.; He, Z.; Wang, S.; Chen, H. Bio-Oil Production from Hydrothermal Liquefaction of Ultrasonic Pre-Treated Spirulina Platensis. *Energy Convers Manag* **2018**, *159*, 204–212, doi:10.1016/j.enconman.2017.12.100.
27. Han, Y.; Hoekman, S.K.; Cui, Z.; Jena, U.; Das, P. Hydrothermal Liquefaction of Marine Microalgae Biomass Using Co-Solvents. *Algal Res* **2019**, *38*, doi:10.1016/j.algal.2019.101421.
28. Tekin, K. Hydrothermal Conversion of Russian Olive Seeds into Crude Bio-Oil Using a CaO Catalyst Derived from Waste Mussel Shells. *Energy and Fuels* **2015**, *29*, 4382–4392, doi:10.1021/acs.energyfuels.5b00724.
29. Vlaskin, M.S.; Grigorenko, A. V.; Kostyukevich, Y.I.; Nikolaev, E.N.; Vladimirov, G.N.; Chernova, N.I.; Kiseleva, S. V.; Popel, O.S.; Zhuk, A.Z. Influence of Solvent on the Yield and Chemical Composition of Liquid Products of Hydrothermal Liquefaction of Arthrospira Platensis as Revealed by Fourier Transform Ion Cyclotron Resonance Mass Spectrometry. *European Journal of Mass Spectrometry* **2018**, *24*, 363–374, doi:10.1177/1469066718771209.
30. Hu, Y.; Wang, S.; Li, J.; Wang, Q.; He, Z.; Feng, Y.; Abomohra, A.E.F.; Afonaa-Mensah, S.; Hui, C. Co-Pyrolysis and Co-Hydrothermal Liquefaction of Seaweeds and Rice Husk: Comparative Study towards Enhanced Biofuel Production. *J Anal Appl Pyrolysis* **2018**, *129*, 162–170, doi:10.1016/j.jaap.2017.11.016.
31. Posmanik, R.; Cantero, D.A.; Malkani, A.; Sills, D.L.; Tester, J.W. Biomass Conversion to Bio-Oil Using Sub-Critical Water: Study of Model Compounds for Food Processing Waste. *Journal of Supercritical Fluids* **2017**, *119*, 26–35, doi:10.1016/j.supflu.2016.09.004.
32. Baloch, H.A.; Siddiqui, M.T.H.; Nizamuddin, S.; Mubarak, N.M.; Khalid, M.; Srinivasan, M.P.; Griffin, G.J. Catalytic Co-Liquefaction of Sugarcane Bagasse and Polyethylene for Bio-Oil Production under Supercritical Conditions: Effect of Catalysts. *J Anal Appl Pyrolysis* **2021**, *153*, doi:10.1016/j.jaap.2020.104944.
33. Carrasco, F.; Chornet, E.; Overend, R.P.; Heitz, M. Fractionnement de Deux Bois Tropicaux (Eucalyptus et Wapa) Par Traitement Thermomécanique En Phase Aqueuse. Partie I: Conversion et Profils de Solubilisation. *Can J Chem Eng* **1986**, *64*, 986–993, doi:https://doi.org/10.1002/cjce.5450640616.
34. Bouchard, J.; Léger, S.; Chornet, E.; Overend, R.P. Quantification of Residual Polymeric Families Present in Thermo-Mechanical and Chemically Pretreated Lignocellulosic via Thermal Analysis. *Biomass* **1986**, *9*, 161–171, doi:https://doi.org/10.1016/0144-4565(86)90086-7.
35. Heitz, M.; Carrasco, F.; Rubio, M.; Chauvette, G.; Chornet, E.; Jaulin, L.; Overend, R.P. Generalized Correlations for the Aqueous Liquefaction of Lignocellulosics. *Can J Chem Eng* **1986**, *64*, 647–650, doi:https://doi.org/10.1002/cjce.5450640416.
36. Rogalinski, T.; Liu, K.; Albrecht, T.; Brunner, G. Hydrolysis Kinetics of Biopolymers in Subcritical Water. *Journal of Supercritical Fluids* **2008**, *46*, 335–341, doi:10.1016/j.supflu.2007.09.037.
37. Melfi, D.T.; Lenzi, M.K.; Ramos, L.P.; Corazza, M.L. Kinetic Modeling of ScCO2-Assisted Levulinic Acid Esterification with Ethanol Using Amberlyst-15 as a Catalyst in a Batch Reactor. *Energy and Fuels* **2021**, *35*, 14770–14779, doi:10.1021/acs.energyfuels.1c01967.
38. Michelsen, M.L.; Mollerup, J.M. *Thermodynamic Models: Fundamentals & Computational Aspects*; 2nd ed.; Tie-Line Publications: Holte, 2007; ISBN 978-8798996118.
39. Tavares, M.V.L.; Giacomin-Junior, W.R.; Vandenberghe, L.P.D.S.; Chapman, W.G.; Corazza, M.L. Phase-Equilibrium Measurements and Thermodynamic Modeling of CO2 + Geraniol, CO2 + Geraniol + Acetic

Preprints.org (www.preprints.org) | NOT PEER-REVIEWED | Posted: 6 June 2024 doi:10.20944/preprints202406.0341.v1

Acid, and CO2 + Geraniol + Ethyl Acetate. *J Chem Eng Data* **2020**, *65*, 1721–1729, doi:10.1021/acs.jced.9b01060.

40. Ramirez, J.A.; Brown, R.J.; Rainey, T.J. A Review of Hydrothermal Liquefaction Bio-Crude Properties and Prospects for Upgrading to Transportation Fuels. *Energies (Basel)* **2015**, *8*, 6765–6794, doi:https://doi.org/10.3390/en8076765.
41. Heidari, M.; Dutta, A.; Acharya, B.; Mahmud, S. A Review of the Current Knowledge and Challenges of Hydrothermal Carbonization for Biomass Conversion. *Journal of the Energy Institute* **2019**, *92*, 1779–1799, doi:https://doi.org/10.1016/j.joei.2018.12.003.
42. Niu, S.; Zhou, Y.; Yu, H.; Lu, C.; Han, K. Investigation on Thermal Degradation Properties of Oleic Acid and Its Methyl and Ethyl Esters through TG-FTIR. *Energy Convers Manag* **2017**, *149*, 495–504, doi:10.1016/j.enconman.2017.07.053.
43. Peters, M.A.; Alves, C.T.; Wang, J.; Onwudili, J.A. Subcritical Water Hydrolysis of Fresh and Waste Cooking Oils to Fatty Acids Followed by Esterification to Fatty Acid Methyl Esters: Detailed Characterization of Feedstocks and Products. *ACS Omega* **2022**, *7*, 46870–46883, doi:10.1021/acsomega.2c05972.
44. Chand, P.; Reddy, C.V.; Venkat, J.G.; Wang, T.; Grewell, D. Thermogravimetric Quantification of Biodiesel Produced via Alkali Catalyzed Transesterification of Soybean Oil. *Energy and Fuels* **2009**, *23*, 989–992, doi:10.1021/ef800668u.
45. Chen, W.T.; Zhang, Y.; Zhang, J.; Schideman, L.; Yu, G.; Zhang, P.; Minarick, M. Co-Liquefaction of Swine Manure and Mixed-Culture Algal Biomass from a Wastewater Treatment System to Produce Bio-Crude Oil. *Appl Energy* **2014**, *128*, 209–216, doi:10.1016/j.apenergy.2014.04.068.
46. Wang, M.; Leitch, M.; Xu, C.C. Synthesis of Phenolic Resol Resins Using Cornstalk-Derived Bio-Oil Produced by Direct Liquefaction in Hot-Compressed Phenol-Water. *Journal of Industrial and Engineering Chemistry* **2009**, *15*, 870–875, doi:10.1016/j.jiec.2009.09.015.
47. Kumar, A.; Negi, Y.S.; Choudhary, V.; Bhardwaj, N.K. Characterization of Cellulose Nanocrystals Produced by Acid-Hydrolysis from Sugarcane Bagasse as Agro-Waste. *Journal of Materials Physics and Chemistry* **2014**, *2*, 1–8, doi:10.12691/jmpc-2-1-1.
48. Leng, L.; Li, J.; Yuan, X.; Li, J.; Han, P.; Hong, Y.; Wei, F.; Zhou, W. Beneficial Synergistic Effect on Bio-Oil Production from Co-Liquefaction of Sewage Sludge and Lignocellulosic Biomass. *Bioresour Technol* **2018**, *251*, 49–56, doi:10.1016/j.biortech.2017.12.018.
49. Mahamuni, N.N.; Adewuyi, Y.G. Fourier Transform Infrared Spectroscopy (FTIR) Method to Monitor Soy Biodiesel and Soybean Oil in Transesterification Reactions, Petrodiesel- Biodiesel Blends, and Blend Adulteration with Soy Oil. *Energy and Fuels* **2009**, *23*, 3773–3782, doi:10.1021/ef900130m.

Disclaimer/Publisher's Note: The statements, opinions and data contained in all publications are solely those of the individual author(s) and contributor(s) and not of MDPI and/or the editor(s). MDPI and/or the editor(s) disclaim responsibility for any injury to people or property resulting from any ideas, methods, instructions or products referred to in the content.